Dystroglycan controls signaling of multiple hormones through modulation of STAT5 activity

Dmitri Leonoudakis[1], Manisha Singh[1], Roozbeh Mohajer[1], Pouya Mohajer[1], Jimmie E. Fata[2], Kevin P. Campbell[3] and John L. Muschler[1,*]

[1]California Pacific Medical Center Research Institute, San Francisco, CA 94107, USA
[2]Department of Biology, College of Staten Island, City University of New York, Staten Island, NY 10314, USA
[3]Howard Hughes Medical Institute, Department of Molecular Physiology and Biophysics, University of Iowa College of Medicine, Iowa City, IA 52242, USA
*Author for correspondence (muschler@cpmcri.org)

Accepted 20 July 2010
Journal of Cell Science 123, 3683-3692

doi:10.1242/jcs.070680

Summary

Receptors for basement membrane (BM) proteins, including dystroglycan (DG), coordinate tissue development and function by mechanisms that are only partially defined. To further elucidate these mechanisms, we generated a conditional knockout of DG in the epithelial compartment of the mouse mammary gland. Deletion of DG caused an inhibition of mammary epithelial outgrowth and a failure of lactation. Surprisingly, loss of DG in vivo did not disrupt normal tissue architecture or BM formation, even though cultured *Dag1*-null epithelial cells failed to assemble laminin-111 at the cell surface. The absence of DG was, however, associated with a marked loss in activity of signal transducer and activator of transcription 5 (STAT5). Loss of DG perturbed STAT5 signaling induced by either prolactin or growth hormone. We found that DG regulates signaling by both hormones in a manner that is dependent on laminin-111 binding, but independent of the DG cytoplasmic domain, suggesting that it acts via a co-receptor mechanism reliant on DG-mediated laminin assembly. These results demonstrate a requirement for DG in the growth and function of a mammalian epithelial tissue in vivo. Moreover, we reveal a selective role for DG in the control of multiple STAT5-dependent hormone signaling pathways, with implications for numerous diseases in which DG function is compromised.

Key words: Dystroglycan, STAT5, Laminin, Mammary, Epithelial, Prolactin, Growth hormone

Introduction

Basement membranes (BMs) are formed adjacent to a wide range of cell types and exhibit diverse functions including the creation of physical barriers between tissue compartments, the provision of structural support to cells and tissues, and the provision of signaling cues for cellular orientation, migration, survival, proliferation and tissue-specific gene expression (Miner and Yurchenco, 2004; Yurchenco et al., 2004). Cell interactions with the BM are mediated by a varied set of receptors that include the β1 and β4 integrins, discoidin domain receptors, syndecans, sulfated glycolipids, Lutheran/BCAM and dystroglycan (Yurchenco and Patton, 2009). However, the distinct and cooperative roles of these receptors remain to be clearly elucidated.

Dystroglycan (DG) functions at virtually all cell–BM interfaces, including those of muscle and epithelial cells, and is present within the peripheral and central nervous systems (Durbeej et al., 1998; Moore et al., 2002; Nishimune et al., 2008). The extracellular domain of DG binds to prominent extracellular matrix proteins, including laminins, perlecan and agrin through O-linked carbohydrate modifications in the α-DG mucin domain (Barresi and Campbell, 2006; Ervasti and Campbell, 1993; Yoshida-Moriguchi et al., 2010). As a nearly ubiquitous extracellular matrix receptor, DG has the potential to have an important role in many developmental processes, and disruption of DG function might contribute to the progression of a diverse range of human diseases.

DG is best known as a central component of the dystrophin–glycoprotein complex (DGC), a multimeric protein complex of the muscle sarcolemma (Durbeej and Campbell, 2002). Genetic loss or depletion of DGC components or DGC-associated proteins is responsible for a large percentage of muscular dystrophies, and DG function itself is ablated or diminished in many of these diseases (Barresi and Campbell, 2006; Cohn and Campbell, 2000). Although genetic defects of the DG coding sequence have not yet been observed in human disease, defects of DG post-translational processing and function have been detected, leading to various muscular dystrophies with associated neurological defects (Barresi and Campbell, 2006). These diseases are rooted in a loss of DG ligand-binding properties in the extracellular domain, resulting from altered carbohydrate modifications, and collectively, have been labeled ‘dystroglycanopathies’ (Muntoni et al., 2008). Defects of DG glycosylation and function resembling those observed in dystroglycanopathies are evident in the progression of many carcinomas (Beltran-Valero de Bernabe et al., 2009; Singh et al., 2004) and appear to contribute to carcinoma progression through altered signaling between cells and the BM (Bao et al., 2009; Beltran-Valero de Bernabe et al., 2009; Muschler et al., 2002; Sgambato et al., 2003).

Conditional and chimeric gene-knockout studies have confirmed that loss of DG expression can recapitulate human disease phenotypes in numerous tissues (Cohn et al., 2002; Cote et al., 1999; Moore et al., 2002; Satz et al., 2008). These studies have established that DG functions in the stabilization of the muscle sarcolemma (Han et al., 2009), basement membrane integrity (Moore et al., 2002), neuromuscular junction maturation (Nishimune et al., 2008) and morphogenesis of the brain and eye (Moore et al., 2002; Satz et al., 2008); however, the precise mechanisms by which DG operates remain unclear.

Journal of Cell Science

Much less is known about DG function in the context of mammalian epithelial cell biology and development. Manipulation of DG in mammalian cell and organ culture supports diverse roles for DG, including roles in epithelial cell survival signaling (Li et al., 2002), branching morphogenesis (Durbeej et al., 2001), epithelial polarization (Muschler et al., 2002; Weir et al., 2006), and tissue-specific gene expression (Weir et al., 2006; Xu et al., 2009). Additionally, DG is crucial for the high-affinity assembly of laminin on the cell surface of cultured mammary epithelial and embryonic stem cells (Henry et al., 2001b; Weir et al., 2006). However, the importance of DG to mammalian epithelial tissue development in vivo is not clear. The conditional deletion of DG from the luminal epithelium of the prostate gland did not produce obvious defects of tissue development or function, but a deletion from the myoepithelial (basal epithelial) compartment of the prostate was not assessed (Esser et al., 2010). As yet, the conditional deletion of *Dag1* gene expression has not been reported for any other adult mammalian epithelial lineage.

Here, we have generated the conditional knockout of DG in the entire epithelial compartment of the mouse mammary gland, including both basal and luminal epithelial cells, and assessed the role of DG in the morphogenesis and function of this epithelial tissue in vivo. These results demonstrate a role for DG in mammary gland outgrowth and function, providing a clear demonstration of tissue defects resulting from the loss of DG within an epithelial cell lineage of adult transgenic mice. Importantly, these results reveal a selective and potent role for DG in the modulation of STAT5 signaling in vivo, with implications for signaling through several STAT5-dependent pathways.

Results

Deletion of *Dag1* gene expression by K14-Cre activity arises in both luminal and basal epithelial cells early in mammary gland development

The conditional knockout of *Dag1* gene expression from the epithelial compartment of the mouse mammary gland was achieved by Cre-*loxP* recombination, crossing the floxed-DG transgenic mouse line (Cohn et al., 2002; Moore et al., 2002) with the K14-Cre line expressing the Cre transgene from the keratin-14 (K14) promoter (Dassule et al., 2000). The K14-Cre transgene has induced DNA recombination that is ultimately detected in both luminal and myoepithelial cell populations of the adult mammary gland, suggesting earlier expression in a common progenitor cell population (Jonkers et al., 2001) but the precise pattern of K14-Cre expression in early mammary gland development has not yet been established. Crossing the K14-Cre transgenic line with the Rosa26R reporter mouse line (Soriano, 1999) revealed K14-Cre-mediated DNA recombination in the mammary buds at day embryonic day 14 (E14) of development (Fig. 1A), coinciding with the earliest invasion of the nascent gland into the mesenchyme (Robinson, 2007). This activity might be initiated just before broader activation of K14-Cre expression in the epidermis at E13.5 (Jonkers et al., 2001) (supplementary material Fig. S1). Cre-induced genetic alteration was perpetuated throughout the developing gland at birth (Fig. 1B) and in the vast majority of mammary epithelial cells, both myoepithelial and luminal, in glands from nulliparous, mid-pregnant and lactating animals (Fig. 1C,D and data not shown).

Mice bearing the floxed *Dag1* locus ($DG^{fl/wt}$ or $DG^{fl/fl}$) were crossed with bi-transgenic mice bearing the floxed DG locus and K14-Cre transgene. The Rosa26R transgene was included in the background of these crosses to permit the visualization of cells that had undergone DNA recombination in Cre-expressing mice. The knockout genotype ($DG^{fl/fl}$; K14-Cre^{+}), abbreviated to $\Delta DG^{K14\text{-}Cre}$, was obtained in ratios consistent with mendelian inheritance. $\Delta DG^{K14\text{-}Cre}$ animals were viable as adults, had comparable body weight to control animals and were fertile. Rosa26R reporter activity was evident throughout the epithelium in mammary glands of $\Delta DG^{K14\text{-}Cre}$ mice (supplementary material Fig. S2). Immunostaining of control tissues, lacking Cre expression, and $\Delta DG^{K14\text{-}Cre}$ mammary tissues confirmed the loss of DG expression (Fig. 2A). In addition, immunoblotting of primary epithelial cultures from control and $\Delta DG^{K14\text{-}Cre}$ mammary glands revealed the virtually complete loss of DG expression from the Cre-expressing glands (Fig. 2B).

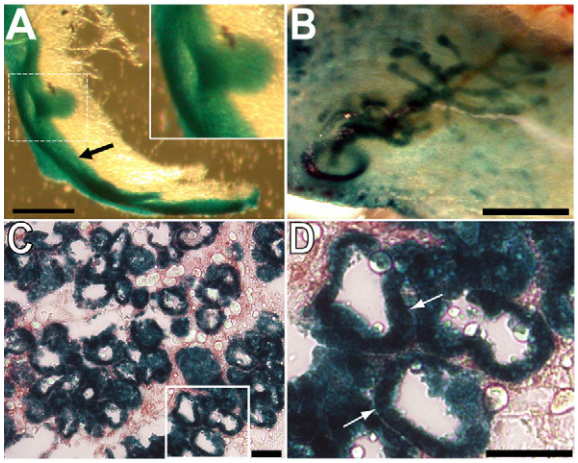

Fig. 1. K14-Cre expression is initiated early in mammary gland development. Histochemical staining for *lacZ* expression was performed in bi-transgenic K14-Cre+; R26R+ mice to reveal K14-Cre-mediated DNA recombination. (**A**) In a transverse view of dissected ventral skin from an E14 embryo, *lacZ* reporter activity (blue) is detected in the epidermal layer (arrow), and in the invaginating mammary bud (box and inset). (**B**) Staining is evident throughout the mammary epithelium at the P1 stage. (**C**) Staining of mammary tissue sections at mid-pregnancy shows widespread *lacZ* expression in the epithelium. (**D**) Enlargement of boxed area in C shows *lacZ* expression in luminal and myoepithelial cell populations (white arrows). Scale bars: 0.2 mm (A), 1 mm (B), 0.5 mm (C) and 50 μm (D).

Loss of DG perturbs epithelial outgrowth and mammary gland function

Mammary gland outgrowth and development was first assessed by whole mount analysis of the fourth (inguinal) gland in nulliparous female mice at 8 weeks of age. In control mice, mammary epithelial outgrowth extended well beyond the central lymph node (Fig. 3A). Comparable outgrowth was observed in heterozygous $DG^{fl/wt;K14\text{-}Cre}$ mice (bearing the K14-Cre and Rosa26R transgenes and $DG^{fl/wt}$ genotype) (Fig. 3B). By contrast, outgrowth of the gland in $\Delta DG^{K14\text{-}Cre}$ mice was impeded, barely surpassing the central lymph node of the inguinal gland (Fig. 3C,D). Despite the impeded outgrowth, epithelial branching occurred and terminal end bud formation was not perturbed.

Lactation is enabled by a dramatic outgrowth of the epithelia during pregnancy, and by lobuloalveolar differentiation. To assess development of DG-knockout mammary glands during pregnancy and lactation, mammary glands were harvested from adult female mice at midpregnancy [day 14.5 post conception (d14.5)] and at

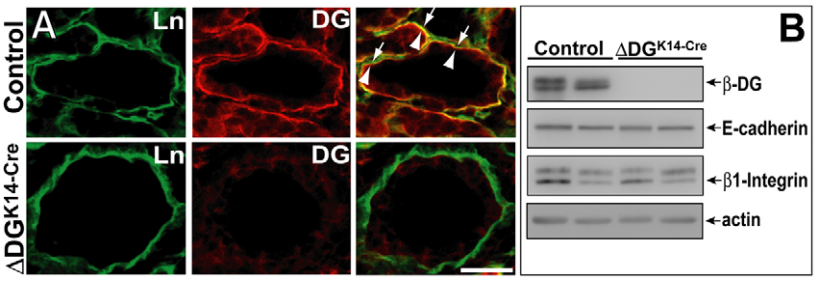

Fig. 2. K14-Cre activity efficiently ablates DG expression. (**A**) Frozen sections of L1 stage mammary glands from control or $\Delta DG^{K14\text{-}Cre}$ mice co-stained with anti-laminin (Ln) and anti-DG (DG) antibodies. The right panels show the merged laminin and DG co-staining. DG staining was absent from the $\Delta DG^{K14\text{-}Cre}$ epithelium. Arrows indicate the green laminin staining the exterior of the gland, whereas arrowheads indicate red DG staining the basal surface of the epithelium. Areas of yellow reveal overlap of laminin with its receptor, DG. Scale bar: 20 µm. (**B**) Protein extracts of primary cell cultures from control and $\Delta DG^{K14\text{-}Cre}$ glands immunoblotted with the antibodies indicated on the right. No β-DG was detected in mammary epithelial cells cultured from $\Delta DG^{K14\text{-}Cre}$ mice.

day 1 of lactation (L1). At mid-pregnancy, control heterozygous, $DG^{fl/wt;K14\text{-}Cre}$ mice exhibited normal outgrowth and development. The glands of mid-pregnant $\Delta DG^{K14\text{-}Cre}$ mice (Fig. 4A) were not discernibly different from control mice. At L1, pups of control and heterozygous, $DG^{fl/wt;K14\text{-}Cre}$ mice were viable; lactation was evident by the appearance of a milk spot in the stomach of pups (supplementary material Fig. S3A) and by their normal growth and maturation. However, in $\Delta DG^{K14\text{-}Cre}$ mice, the majority of mothers demonstrated a failure of lactation, with pups dying within 1 day of birth. Despite active nursing, the pups appeared emaciated and a milk spot did not appear (supplementary material Fig. S3B), indicating that the mothers failed to produce sufficient quantities of milk. Of 29 $\Delta DG^{K14\text{-}Cre}$ females giving birth, 15 (52%) failed at the stage of lactation. Of these 15 mothers, 12 failed to support the survival of any pups, and three were able to support through maturation only two or three pups from initial litters of six or more. The defect of lactation was not reversed by subsequent pregnancies; mice that failed in lactation with first litters also failed with subsequent litters.

Whole-mount analysis revealed that the growth of mammary glands in $\Delta DG^{K14\text{-}Cre}$ mothers at the L1 stage had not progressed significantly beyond that seen at d14.5 of mid-pregnancy (Fig. 4B and supplementary material Fig. S4). This contrasted with control tissues, which displayed extensive growth and expansion of the lobuloalveolar units. Quantification of L1 mammary gland whole mounts demonstrates a 20% decrease in gland growth (Fig. 4C). Despite the impeded outgrowth of the gland, expression of milk protein genes was not disrupted in lactating $\Delta DG^{K14\text{-}Cre}$ mice (supplementary material Fig. S5).

DG loss disrupts laminin assembly at the epithelial cell surface but does not perturb epithelial cytoarchitecture or basement membrane formation in vivo

DG has been implicated in cell-surface laminin assembly and polarity signaling in assays using immortalized mammary epithelial cells (Muschler et al., 2002; Weir et al., 2006). In primary cultures, laminin assembled extensively at the surface of mammary epithelial cells from control animals (Fig. 5A), and similar assembly was observed in immortalized mammary epithelial cell lines (Fig. 5B). In cultures from $\Delta DG^{K14\text{-}Cre}$ animals, significant laminin assembly was absent (Fig. 5A), replicating results obtained in immortalized cell lines lacking DG expression (Fig. 5B) (Weir et al., 2006). Quantification in primary cultures of control and $\Delta DG^{K14\text{-}Cre}$ mammary epithelial cells revealed greater than 80% reduction in the assembly of laminin in DG-knockout cells (Fig. 5C). Surprisingly, despite this defect observed in primary cultures, mammary glands from $\Delta DG^{K14\text{-}Cre}$ animals did not exhibit changes in tissue cytoarchitecture or basement membrane formation in vivo. Immunostaining for epithelial polarity markers in tissue sections from $\Delta DG^{K14\text{-}Cre}$ mammary glands showed normal distribution of the tight junction protein ZO-1 at the apical surface and α6 integrin at the basal surface (supplementary material Fig. S6A). Immunostaining with myoepithelial markers showed a comparable distribution of luminal and myoepithelial cells in the

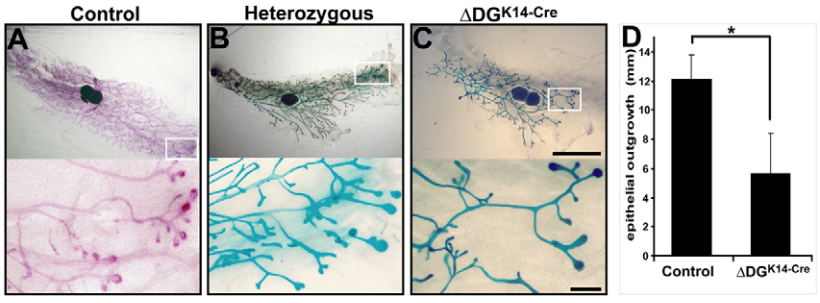

Fig. 3. Knockout of dystroglycan expression in the mammary gland impedes growth of the epithelial compartment. Mammary gland development in control and $\Delta DG^{K14\text{-}Cre}$ was assessed by whole-mount staining of the fourth (inguinal) gland isolated from nulliparous females at 8 weeks of age. (**A**) Control glands stained with Carmine Alum. (**B**) Glands from heterozygous ($DG^{fl/wt;K14\text{-}Cre}$) and (**C**) $\Delta DG^{K14\text{-}Cre}$ mice stained with X-gal when the Rosa26R transgene was present, revealing Cre activity. The lymph node appears as dark circles at the center of the gland. Lower panels are enlarged portions (white boxes) of the images above. Scale bars: 5 mm (top) and 500 µm (bottom). (**D**) Outgrowth of the mammary gland beyond the central lymph node measured for glands of 8-week-old control (n=6) and $\Delta DG^{K14\text{-}Cre}$ (n=4) mice. *P<0.005.

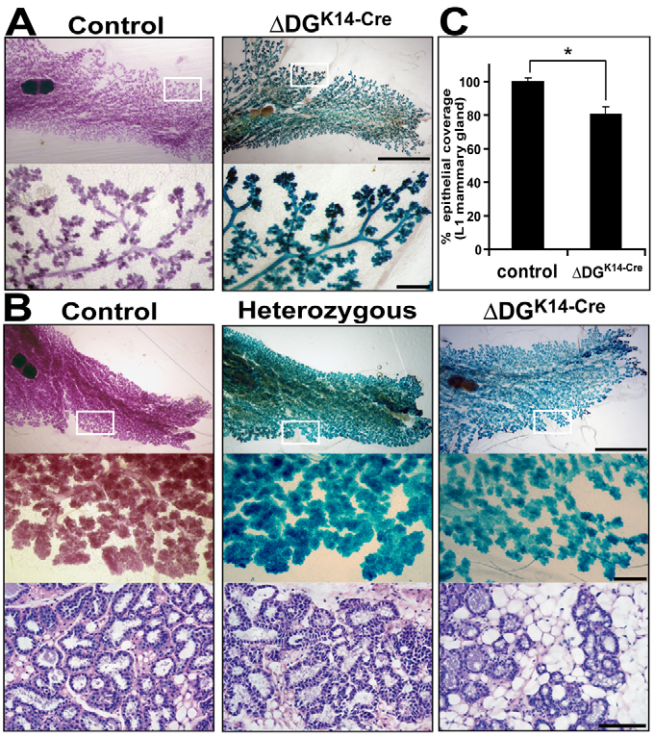

Fig. 4. Mammary gland outgrowth is attenuated after mid-pregnancy in ΔDG$^{K14\text{-}Cre}$ mice. Mammary gland development in control and knockout mice was assessed by whole mount staining of fourth (inguinal) gland and by hematoxylin and eosin staining of tissue sections. Control glands are stained with Carmine Alum whereas heterozygous and ΔDG$^{K14\text{-}Cre}$ glands are stained with X-gal, revealing Cre activity on the Rosa26R transgene. (**A**) ΔDG$^{K14\text{-}Cre}$ glands at mid-pregnancy (day 14.5) show normal tissue architecture and outgrowth compared with control glands. Scale bars: 5 mm (top) and 500 μm (bottom). (**B**) At lactation day 1 (L1), heterozygous DG glands show normal tissue architecture, whereas ΔDG$^{K14\text{-}Cre}$ glands display an apparent reduction in outgrowth. Scale bars: 5 mm (top), 500 μm (middle) and 100 μm (bottom). (**C**) Digital images of whole-mount L1 mammary glands traced and thresholded to determine percentage epithelial coverage. Compiled data reveal a 20% reduction in ΔDG$^{K14\text{-}Cre}$ epithelial outgrowth (n=3; *P<0.05).

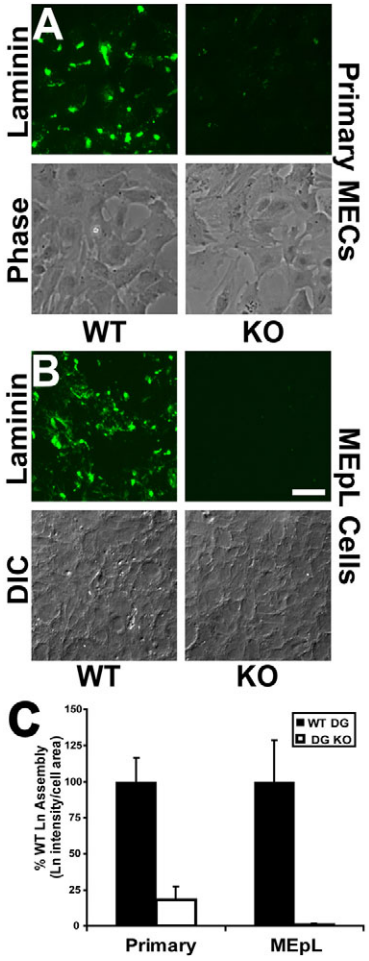

Fig. 5. Laminin assembly is compromised in mammary epithelial cells lacking DG expression. (**A**) Primary mammary epithelial cells from control or ΔDG$^{K14\text{-}Cre}$ mice were incubated with 10 ng/ml FITC-laminin-111 overnight. DG-expressing cells (WT) showed efficient assembly of laminin, whereas DG-knockout cells (KO) showed little assembled laminin. The phase-contrast images below show the positions of the cells. (**B**) Cells derived from the immortalized DG-knockout cell line (MEpL), transfected with DG (WT) or a vector control (KO) were overlaid with 10 ng/ml FITC-laminin-111 overnight. WT cells show efficient assembly of laminin, whereas the knockout cells show no assembled laminin. The differential interference contrast images below show the positions of the cells. Scale bar: 10 μm. (**C**) Fluorescence images as in A and B were thresholded and the resulting pixel intensity was divided by the cell area. The compiled quantified data are normalized to WT. Data were compiled from two experiments and 10 images each. P<0.0001 for both primary mammary epithelial cells and MEpL cells (error bars indicate s.e.m.).

tissues of control and ΔDG$^{K14\text{-}Cre}$ mice, indicating no significant changes to the myoepithelial lineage (supplementary material Fig. S6B). Epithelial compartments lacking DG expression were surrounded by a continuous basement membrane, as evidenced by laminin staining, which appeared to be of normal integrity and thickness (Fig. 2 and supplementary material Fig. S6C).

DG is crucial for STAT5 activity in vivo

Outgrowth and function of the mammary gland is strongly influenced by growth hormone and prolactin signaling (Kelly et al., 2002), and by signaling from extracellular matrix receptors of the β1 integrin family (Li et al., 2005; Naylor et al., 2005). A shared downstream target of these extracellular signals is the activation of the transcription factor signal transducer and activator of transcription 5 (STAT5) (Cui et al., 2004; Hennighausen and Robinson, 2008; Naylor et al., 2005). Deletion of STAT5 expression in the mammary gland causes inhibited outgrowth and function that resembles the phenotype we observed in the ΔDG$^{K14\text{-}Cre}$ mammary gland, although it is more severe in the STAT5-knockout animals (Cui et al., 2004; Liu et al., 1997). To test whether STAT5 functions were perturbed in the absence of DG in vivo, STAT5 activation was assayed in L1 stage mammary glands of control and ΔDG$^{K14\text{-}Cre}$ mice by immunostaining for its nuclear localization using an anti-STAT5 antibody, and by immunostaining directly for active STAT5 using an anti-phospho-STAT5 antibody. Immunostaining for total STAT5 in lactating tissues showed the presence of STAT5 in the mammary epithelial cells from both control and ΔDG$^{K14\text{-}Cre}$ mice; however, there was a clear exclusion of STAT5 from the nucleus in the epithelial cells of ΔDG$^{K14\text{-}Cre}$ mice, which indicated a decrease in STAT5 activation (Fig. 6A). Immunostaining specifically for phosphorylated STAT5 (P-STAT5)

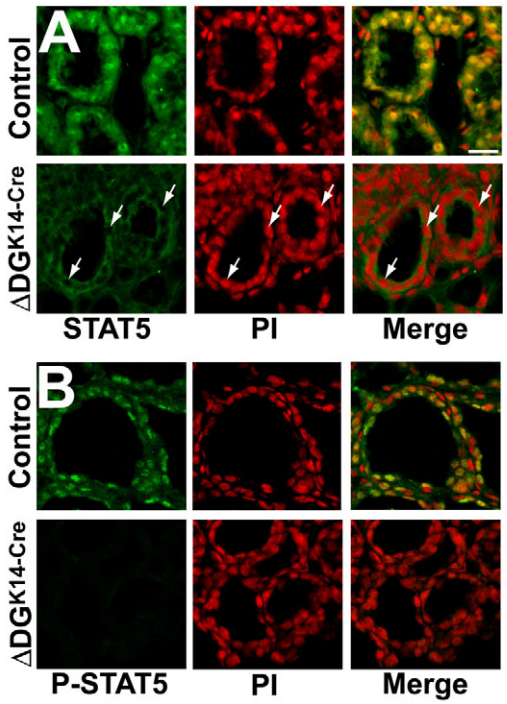

Fig. 6. DG modulates STAT5 activity in vivo. (**A**) Frozen sections of L1 stage mammary glands from control or $\Delta DG^{K14\text{-}Cre}$ mice immunostained with anti-STAT5 antibodies and counterstained with propidium iodide. $\Delta DG^{K14\text{-}Cre}$ mammary glands show markedly reduced nuclear STAT5 staining as indicated by the arrows and lack of overlap staining (yellow color) in the merged images at right. (**B**) Frozen sections of L1 stage mammary glands from control or $\Delta DG^{K14\text{-}Cre}$ mice immunostained with anti-P-STAT5 antibodies and counterstained with propidium iodide. P-STAT5 staining in $\Delta DG^{K14\text{-}Cre}$ mammary glands is absent. Scale bar: 20 µm.

revealed an even more striking difference. In control tissues, P-STAT5 was clearly evident and enriched in the nuclei of luminal epithelial cells (Fig. 6B). In the glands of $\Delta DG^{K14\text{-}Cre}$ mice, P-STAT5 staining was very weak, confirming a dramatic loss of STAT5 activity in the absence of DG. Loss of nuclear STAT5 and P-STAT5 staining was also observed in 8-week-old nulliparous mice, coinciding with the impeded outgrowth observed at this stage (supplementary material Fig. S7).

DG modulates growth-hormone-induced STAT5 activity

STAT5 mediates signaling from several hormones and cytokines, which, in the mammary gland, include both prolactin and growth hormone. Disruption of prolactin receptor signaling can explain the defect of outgrowth during pregnancy, but not the observed defect of outgrowth in nulliparous females (Oakes et al., 2008). If DG acts at the level of STAT5 activation, then loss of STAT5 activation in the $\Delta DG^{K14\text{-}Cre}$ mammary gland could also obstruct signaling through the growth hormone receptor, contributing to defects of outgrowth in both nulliparous and pregnant animals. This was tested using paired, DG-knockout and DG-expressing mammary epithelial cells that were established previously from $DG^{fl/fl}$ mice (MEpL cells) (Weir et al., 2006). To activate both DG and STAT5 signaling pathways, prolactin or growth hormone were added to these cells cultured in three-dimensional (3D) gels of reconstituted basement membrane (rBM) proteins. Immunostaining for P-STAT5 in the cell nuclei showed clear STAT5 activation in the DG-expressing cells following 24 hours exposure to either prolactin or growth hormone; but STAT5 activation was attenuated in DG-knockout cells (Fig. 7A). The levels of STAT5 activation were quantified by immunoblotting for P-STAT5 and total STAT5 in each cell population (Fig. 7B). This revealed that sustained activation of STAT5 was significantly diminished in DG-knockout cells; reduced by 62% for prolactin and 47% for growth hormone (Fig. 7C). Quantitative PCR (qPCR) measurements of β-casein and whey acidic protein (WAP) gene expression, which are both induced by STAT5 activation in mammary epithelial cells, also revealed a strong reduction in signaling induced either by prolactin (reduced by 81% and 90%, respectively) or growth hormone (reduced by 25% and 65%, respectively) in DG-knockout cells (Fig. 7D,E), mirroring the direct assays of activated STAT5. Similarly, induction of IGF-1 expression by prolactin or growth hormone signaling was very strongly attenuated in DG-knockout cells (by 96% in both cases) (Fig. 7F). These data demonstrate by several measures that DG modulates STAT5 activity induced either by prolactin or growth hormone receptor signaling in a cell autonomous manner.

The modulation of prolactin receptor signaling by the extracellular matrix, specifically laminin-111, has previously been established in cultured mammary epithelial cells (Streuli et al., 1995). The relationship of DG to growth hormone signaling presented above suggests these same relationships established for prolactin receptor signaling will also hold true for growth hormone receptor signaling. To test the dependence of growth hormone receptor signaling on laminin-111, MEpL cells expressing wild-type DG were plated on plastic and overlayed with rBM proteins or purified laminin-111, and stimulated with growth hormone for 72 hours. Immunoblotting extracts from these cells revealed a greater than twofold increase in the induction of the milk protein β-casein in the presence of rBM proteins or purified laminin when compared with GH treatment alone (Fig. 8A). Additionally, qPCR analysis of *Igf1* mRNA induction by GH also revealed a greater than twofold increase in *Igf1* expression (Fig. 8B), again confirming modulation by laminin-111.

Previously, we demonstrated that DG can mediate prolactin signaling in a manner that is independent of the DG cytoplasmic domain, through laminin-111 binding and assembly in an apparent co-receptor relationship with β1 integrins (Weir et al., 2006). To test whether the cytoplasmic domain of DG is necessary for the modulation of growth hormone signaling, MEpL cells expressing wild-type DG or DG with the entire cytoplasmic domain deleted (ΔC; residues 780–895) were grown on 3D gels of rBM proteins and stimulated with prolactin or growth hormone for 24 hours. Analysis of activated STAT5 signaling with an anti-P-STAT5 antibody revealed that MEpL cells expressing the ΔC DG construct modulated both prolactin and growth hormone receptor signaling as efficiently as was observed with wild-type DG (Fig. 9A,B). Immunoblotting extracts from these cells revealed greater than 6.5-fold induction of β-casein with prolactin and fivefold more with growth hormone (β-casein to E-cadherin ratios of wild-type and ΔC versus knockout MEpL cells) when comparing the wild type or ΔC MEpL cells with DG-knockout cells (Fig. 9A). Additionally, growth hormone induction of *Igf1* transcript through the ΔC DG construct was as efficient as wild-type DG (Fig. 9C) as determined by qPCR. These data demonstrate that laminin-induced regulation of hormone signaling requires the extracellular but not cytoplasmic domain of dystroglycan.

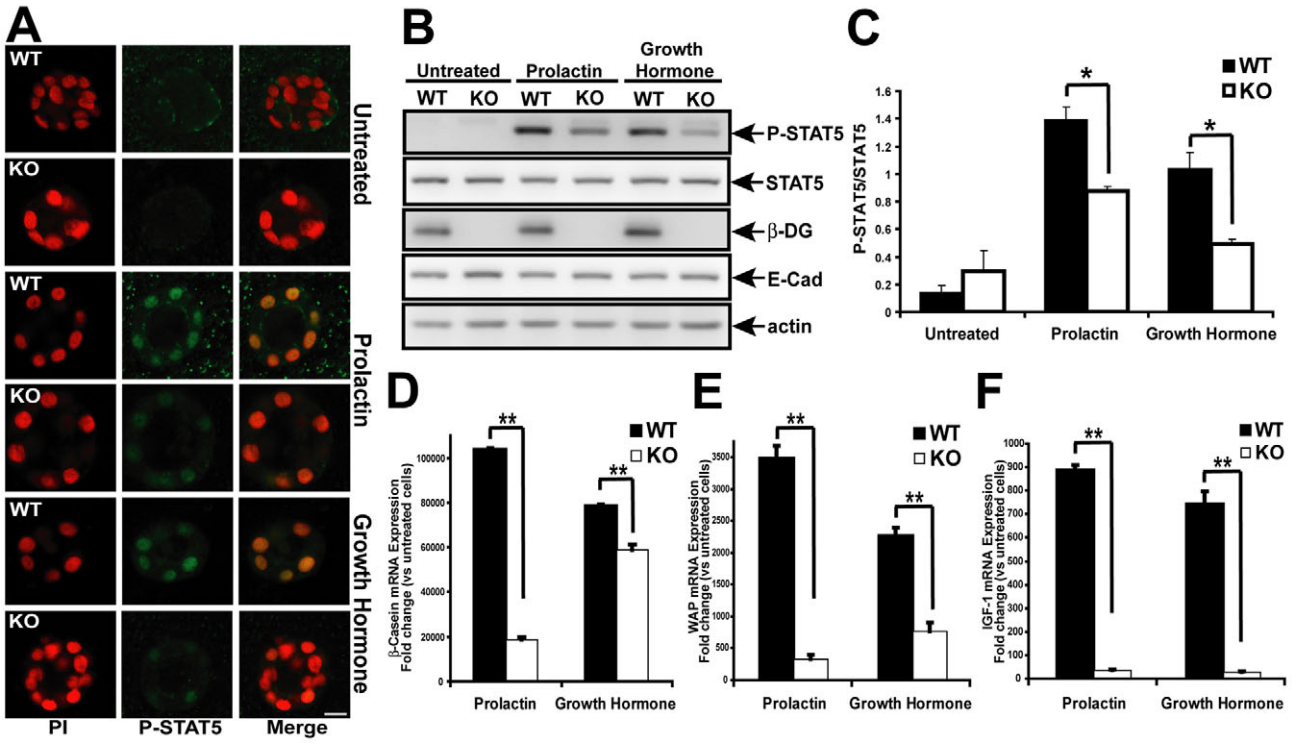

Fig. 7. Loss of DG attenuates prolactin and growth hormone signaling through STAT5. (**A**) Immortalized mammary epithelial cells (MEpL cells) lacking DG expression (KO) or expressing the wild-type DG cDNA (WT) were grown in 3D rBM cultures for 1 week and treated with prolactin or growth hormone or left untreated for 24 hours. Cell colonies were stained with anti-P-STAT5 antibodies and nuclei counterstained with propidium iodide. Confocal images show staining of nuclear P-STAT5. Scale bar: 10 μm. (**B**) Protein extracts from MEpL cells grown in 3D cultures and stimulated with hormones immunoblotted with the antibodies indicated on the right. (**C**) Ratio of P-STAT5 to STAT5 quantified from immunoblots as in B (*P<0.05, n=3; error bars indicate s.e.m.). (**D**–**F**) Total RNA was extracted from MEpL cells grown and treated as above for 24 hours (D,E) or 72 hours (F). Real time-qPCR was performed for the expression of genes encoding β-casein, WAP and IGF-1 and normalized to *Gapdh* expression. Data are expressed as the fold change of mRNA in hormone-treated samples versus untreated samples (**P<0.001; error bars indicate s.d.).

Discussion

The multifaceted functions of given proteins are often exposed by exploring their activities in distinct, tissue-specific contexts. We report here the direct assessment of DG knockout in an adult mammalian epithelial tissue, revealing a vital role for DG in the growth and function of the mammary gland. Among the many functions attributed to DG from cell and organ cultured studies, this in vivo work asserts a clear and important role for DG in the control of STAT5 signaling. STAT5 activity was markedly reduced in mammary epithelial cells lacking DG. Loss of STAT5 activation was evidenced by nuclear exclusion of total STAT5, and by loss of P-STAT5 signals in immunostained tissue sections, and was evident at all stages of adult mammary gland development. Moreover, mammary glands of $\Delta DG^{K14\text{-}Cre}$ mice exhibited a reduced outgrowth during pregnancy, resulting in a failure of mothers to adequately nourish their pups. The phenotype appears to be caused by reduced outgrowth because there is no evidence of premature involution, as measured by changes in STAT3 activity (supplementary material Fig. S8) (Philp et al., 1996). This defect of mammary gland outgrowth and function in the $\Delta DG^{K14\text{-}Cre}$ mice resembles a milder form of the phenotypes obtained with the mammary-gland-specific knockouts of STAT5a, STATa/b and the STAT5 activator JAK2 (Cui et al., 2004; Liu et al., 1997; Wagner et al., 2004). A milder phenotype than that observed in STAT5-knockout mice would be anticipated in the $\Delta DG^{K14\text{-}Cre}$ mice because STAT5 activity is reduced but not eliminated, as observed in cultured DG-knockout cells (Figs 7 and 9). This convergence of phenotypes in the DG, STAT5 and JAK2 knockouts is, therefore, evidence of a selective and important role for DG in the modulation of STAT5 activity.

K14-Cre-mediated knockout of DG modifies both myoepithelial and luminal cells of the mammary gland, therefore, DG loss in myoepithelial cells might also contribute to the observed phenotype. For example, loss of oxytocin signaling in myoepithelial cells can also lead to a decrease in STAT5 activation at L1, failed lactation and a decrease in post partum mammary gland development at L3 (Wagner et al., 1997). We cannot rule out possible effects on oxytocin signaling in the failed lactation. However, disruption of oxytocin signaling would not appear to explain the loss of epithelial outgrowth observed in $\Delta DG^{K14\text{-}Cre}$ mice at 8 weeks of age or at the L1 stage, and does not explain the cell-autonomous modulation of STAT5 activity by DG that was observed in cell culture. All the same, DG function is known to stabilize the muscle sarcolemma (Han et al., 2009), and the potential exists for important functions of DG in the contractile myoepithelial cell population.

Laminin-111 signaling is known to regulate prolactin receptor signaling in cultured mammary epithelial cells (Streuli et al., 1995) and has been shown recently to act by maintaining sustained STAT5 activation (Xu et al., 2009). The results we present here provide in vivo evidence that DG participates in the pathway

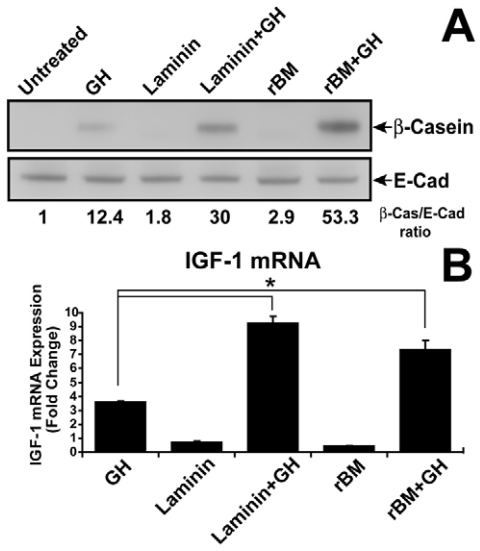

Fig. 8. Laminin-111 enhances the expression of genes induced by growth hormone. MEpL cells expressing WT DG were overlaid with medium containing 100 μg/ml laminin-111 or 1.5% matrigel in the presence or absence of growth hormone for 72 hours. (**A**) Cell lysates were analyzed for the presence of the milk protein β-casein by western blot. E-cadherin was used as a loading control. The ratio of β-casein to E-cadherin was normalized to untreated cells and is indicated below the immunoblots. (**B**) Total RNA was extracted from these cells and RT-qPCR was performed for the expression of *Igf1* and normalized to *Gapdh* expression. The data is expressed as the fold change of mRNA in hormone-treated samples versus control, untreated samples (**P*<0.01; error bars indicate s.d.).

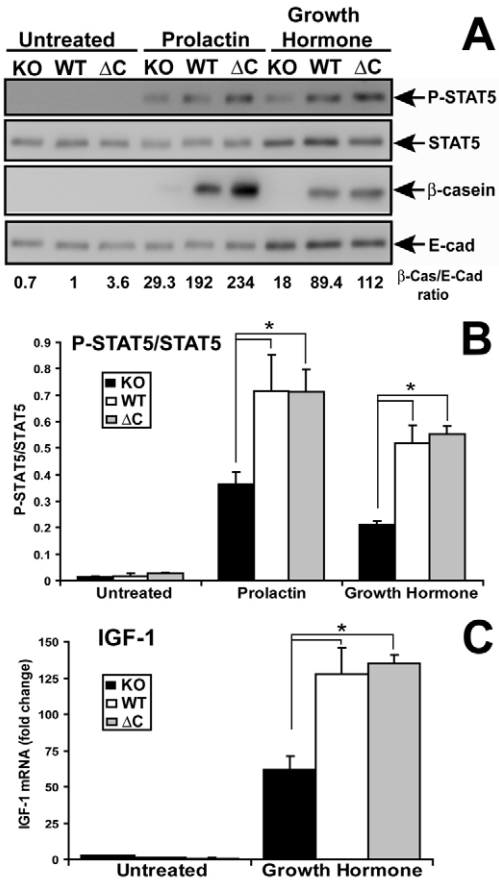

Fig. 9. The cytoplasmic domain of dystroglycan is not required for modulation of STAT5 activity or expression of genes induced by prolactin and growth hormone. MEpL cells lacking DG expression (KO), expressing the wild-type DG cDNA (WT) or intracellular C-terminal deletion mutant of DG (ΔC) were grown in 3D rBM cultures for 1 week and treated with prolactin or growth hormone for 24 hours. (**A**) Protein extracts from MEpL cells grown in 3D cultures and stimulated with hormones were immunoblotted with the antibodies indicated on the right. E-cadherin was used as a loading control. The ratio of β-casein to E-cadherin was normalized to WT DG, untreated cells and is indicated below the immunoblots. (**B**) Ratio of P-STAT5 to STAT5 quantified from immunoblots as in A (**P*<0.05, *n*=3; error bars indicate s.e.m.). (**C**) Total RNA was extracted from MEpL cells grown and treated as above. RT-qPCR was performed for the expression of *Igf1* and normalized to *Gapdh* expression. The data is expressed as the fold change of mRNA in hormone-treated samples versus control, untreated sample and normalized to the WT DG untreated sample (**P*<0.05, error bars indicate s.d.).

between laminin binding at the cell surface and the sustained activation of STAT5. Importantly, we also demonstrate that the influence of basement membranes on STAT5 activation is not confined to prolactin-mediated signals, but can now be expanded to growth hormone signaling and probably that of other hormones and cytokines that signal through STAT5. To our knowledge, DG and cell interactions with the basement membrane have never before been implicated in the control of growth hormone signaling. However, this relationship has been presaged by previous animal studies where a strong inhibition of postnatal growth is evident in mice lacking DG functions (Lee et al., 2005; Levedakou et al., 2005; Satz et al., 2008) or laminin-α2 expression (Miyagoe et al., 1997). Thus far, this inhibition of postnatal growth has lacked an adequate molecular explanation, but it mirrors the phenotype obtained from the loss of STAT5 activity and growth hormone signaling in transgenic mice (Klover and Hennighausen, 2007).

The mechanism by which DG initiates signals from laminins is uncertain, but evidence increasingly points to a co-receptor mechanism and not a direct signaling function (Weir et al., 2006; Yurchenco et al., 2004). This conclusion is based largely on our demonstration that the cytoplasmic domain of DG is not essential to DG-mediated control of prolactin and growth hormone signaling; thus suggesting a model whereby DG operates as a co-receptor through anchorage and assembly of laminin at the cell surface (Weir et al., 2006). The role of DG in cell-surface laminin-111 assembly was demonstrated previously using embryonic stem cells and immortalized mammary epithelial cells (Henry and Campbell, 1998; Weir et al., 2006), and confirmed again here using primary mammary epithelial cultures. The precise mechanism of this proposed co-receptor function remains to be elucidated. DG might alter laminin conformation or, alternatively, DG-mediated laminin assembly might alter the mechanical properties of the basement membrane and modify mechanosignal transduction via co-receptors. In either case, it is evident from our results that the presence of the BM alone is not sufficient for proper STAT5 regulation, but appears to rely instead on a specific organization of BM components, conferred by dystroglycan.

The β1 integrin receptor family has also been implicated in laminin signaling in mammary epithelial cells (Muschler et al., 1999; Naylor et al., 2005; Streuli et al., 1995), and is a leading candidate for a signaling co-receptor for DG in the laminin-STAT5 regulatory

axis. According to the DG–integrin co-receptor model, DG functions in the same pathway as laminin-binding β1 integrins. In this light, it is significant that the DG knockout phenotype in the mammary gland mimics the knockout phenotypes observed for β1 integrins, and the integrin-associated kinases integrin-linked kinase (ILK) and focal adhesion kinase (FAK). Similarly to the DG knockout, β1 integrin, ILK and FAK knockouts each cause a failure of epithelial outgrowth and function in the mammary gland, and each perturbs STAT5 activity (Akhtar et al., 2009; Nagy et al., 2007; Naylor et al., 2005), providing genetic support in vivo for the hypothesized co-receptor relationship between DG and β1 integrin.

The β1 integrins and DG are nearly ubiquitous extracellular matrix receptors, and are co-expressed in all cell types exposed to laminins. Therefore, the proposed co-receptor relationship between DG and β1 integrins in laminin signaling might operate in many different tissues. Similarly, STAT5 is the most widely expressed of the STAT proteins, with known functions in epithelia, muscle tissues, liver, the immune system and the central nervous system (Hennighausen and Robinson, 2008). Observation of the potent influence of laminin, DG and integrins on the regulation of STAT5 activity in the mammary gland suggests that this co-receptor-initiated pathway of STAT5 regulation could be operational in many normal developmental processes. The disruption of this pathway and loss of STAT5 activation might explain human disease manifestations, including unexplained pathologies of the eye and brain that accompany congenital muscular dystrophies. Notably, a close relationship between DG and integrin signaling has been observed in the brain where, similarly to our observations in the mammary gland, there is a convergence of phenotypes observed among the conditional knockouts of DG, β1 integrin, FAK and ILK, where each exhibits defects of cortical organization (Beggs et al., 2003; Graus-Porta et al., 2001; Moore et al., 2002; Niewmierzycka et al., 2005; Satz et al., 2008). Similar CNS abnormalities are observed in mouse models of congenital muscular dystrophies originating from defects in laminin-α2, α7β1 integrin or DG function (Lee et al., 2005; Levedakou et al., 2005; Miyagoe et al., 1997; Satz et al., 2008), and are reflected in human congenital muscular dystrophy patients with defects of laminin-α2 and DG (Reed, 2009). Correspondingly, mice expressing hypomorphic *Stat5* alleles demonstrate defects of cell proliferation and neural migration in the CNS (Hennighausen and Robinson, 2008; Markham et al., 2007), portending that loss of STAT5 activity can underlie CNS defects of congenital muscular dystrophies.

Altered interactions between cells and the basement membrane are also strongly implicated in the progression of many cancers, including those of the breast (Bissell et al., 2002). Importantly, loss of DG function is evident in many carcinomas, including breast cancer (Henry et al., 2001a; Muschler et al., 2002) and in the progression of other cancer types, including gliomas and pediatric cancers (Calogero et al., 2006; Martin et al., 2007). Because DG is a mediator of normal cell and basement membrane interactions and is lost in tumor progression, it is hypothesized to possess tumor suppressor functions, which is supported by cell behavior assays in normal and cancerous cells (Bao et al., 2009; Beltran-Valero de Bernabe et al., 2009; Muschler et al., 2002; Sgambato et al., 2004; Weir et al., 2006). The role of DG in the regulation of STAT5 activity revealed here adds a new dimension to the potential role of DG in cancer progression through support of growth hormone and prolactin signaling, IGF-1 production and growth stimulation (Cotarla et al., 2004; Tan and Nevalainen, 2008).

Materials and Methods

Generation of mice with mammary-epithelial-specific knockout of dystroglycan

The floxed DG mouse line has been previously described (Moore et al., 2002). The transgenic mouse lines K14-Cre [Tg (KRT 14-cre) 1Amc/J, 004782] and Rosa26 [B6.129S4-Gt(Rosa)26Sor^{tm1Sor}/J, 003474] were obtained from The Jackson Laboratory (Bar Harbor, ME). All lines used in this study were backcrossed into the C57BL/6 background more than six times before analysis. Female mice of more than 8 weeks of age were crossed and glands were harvested at midpregnancy [day 14.5 post conception (d14.5)] and at day 1 of lactation (L1). Loss of DG expression in the epidermis via K14-Cre activity did not produce any blistering or overt skin disease, and there were no apparent adverse effects on the health or longevity of the animals (data not shown). All animal use was reviewed and approved by the Institutional Animal Care and Use Committee of the California Pacific Medical Center Research Institute.

Histochemistry

Dissected glands were fixed for 30 minutes in 2% paraformaldehyde in PBS, 0.1% NP-40, washed in PBS, and stained with X-gal solution overnight at room temperature. Carmine Alum staining was performed following fixation in Carnoy's solution. Paraffin embedding, sectioning and staining with hematoxylin and eosin were performed by the Histopathology Reference Laboratory (Hercules, CA). Outgrowth of the mammary gland in nulliparous mice was quantified by measuring the distance from the central lymph node to the tip of the most distal epithelial structure. The percentage epithelial coverage at L1 was calculated from images of mammary gland whole mounts in supplementary material Fig. S4 using Metamorph software (Molecular Devices). The outside edge of the epithelium extending beyond the lymph node was traced and thresholded to include only epithelium. The thresholded area was then divided by the total area. The ratio in control samples was designated as 100% epithelial coverage.

Cell culture

Primary mammary epithelial cells from control or $\Delta DG^{K14\text{-}Cre}$ midpregnant mice were obtained as previously described (Weir et al., 2006). DG-knockout, DG-expressing mammary epithelial cells (MEpL cells) and the cytoplasmic DG deletion (ΔC) were established previously from $DG^{fl/fl}$ mice (Weir et al., 2006) and grown in DME/F12, 2% FBS, 10 μg/ml insulin, 5 ng/ml EGF (BD Biosciences). For culture of rBM proteins on 3D gels, plastic plates were coated with a thin layer of Matrigel (BD Biosciences). The following day medium was replaced with new medium containing 1.5% Matrigel in suspension. After 1 week, the medium was replaced with serum-free medium without EGF but with 0.5 μg/ml hydrocortisone. The following day, either sheep prolactin (3 μg/ml) (Sigma) or mouse growth hormone (1 μg/ml) (National Hormone and Peptide Program, Torrance, CA) was added. 24 hours later, cells were harvested for assessment of STAT5 activation. For biochemistry, cells were isolated from Matrigel in cold PBS with 5 mM EDTA as described (Xu et al., 2009).

Biochemistry and SDS-PAGE

Cells were lysed in RIPA lysis buffer (50 mM Tris-HCl, pH 8.0, 1% NP-40, 0.5% deoxycholate, 0.1% SDS, 1 mM EDTA, 1 mM EGTA 1 mM PMSF, 50 mM NaF, 100 mM $Na_4P_2O_7$, 10 mM Na β-glycerophosphate, 1 mM Na_3VO_4, 1× protease inhibitor cocktail-Chemicon) and quantified with the DC protein assay (Bio-Rad). 10 μg of extracted proteins were resolved on SDS-PAGE gels, transferred to PVDF membranes (Immobilon-P) (Millipore) and immunoblotted as described (Weir et al., 2006). The following primary antibodies were used for immunoblotting: 1:250 rabbit anti-P-STAT5 (Invitrogen), 1:500 rabbit anti-STAT5 (Santa Cruz Biotechnology), 1:5000 rabbit anti-actin (Sigma), 1:2000 mouse E-cadherin (BD Transduction Labs), 1:2000 mouse β-DG (MANDAG-2, Developmental Studies Hybridoma Bank, Iowa), 1:1000 mouse β1 integrin (PharMingen). HRP-conjugated secondary antibodies specific for rabbit and mouse IgG (Jackson ImmunoResearch) were used at 1:15,000. Immunoblot signals were visualized by enhanced chemiluminescence (Super Signal West Femto, Pierce, Rockford, IL) and digitally imaged with an Alpha Innotech imager (San Leandro, CA). Before image processing, bands were quantified using Alpha Ease EC analysis software (Alpha Innotech). Figures are inverted images processed with Adobe Photoshop.

Immunofluorescence microscopy of tissue sections

Dissected mammary gland tissue was embedded in OCT (Tissue-Tek) and frozen on dry ice. 10-μm-thick sections were cut with a cryostat, transferred to charged slides, and fixed in 100% methanol for 20 minutes at –20°C, washed with PBS, and blocked with 3% BSA, 2% goat serum, 0.2% Triton X-100 (Sigma) in PBS (blocking buffer) for 1 hour. Sections were then incubated overnight at 4°C with the following primary antibodies diluted in blocking buffer: 1:100 rabbit anti-ZO-1 (Zymed), 1:200 rabbit anti-laminin, 1:50 rabbit anti-P-STAT5 (Invitrogen), 1:50 rabbit anti-STAT5 (Santa Cruz Biotechnology), 1:1000 rabbit anti-keratin-14 (Sigma), 1:30 rat GoH3 mAb anti-α6-integrin (Chemicon), 1:50 mouse anti-β-DG (MANDAG-2, Developmental Studies Hybridoma Bank, Iowa), 1:400 mouse anti-α-smooth-muscle-actin (clone 1A4, Sigma), 1:200 mouse E-cadherin (BD Transduction Labs). Sections were washed three times with PBS, stained for 1 hour with the following secondary

antibodies diluted in blocking buffer: 1:50 goat anti-rabbit-FITC, 1:200 goat anti-mouse-CY3 (Jackson ImmunoResearch) or 1:200 goat anti-rabbit-Rhodamine. Sections were then washed three times in PBS and mounted with Fluoromount G (Electron Microscopy Sciences) and a coverslip. Sections stained for P-STAT5 or STAT5 were counterstained with 10 μg/ml propidium iodide (Sigma) to stain the nuclei. For staining with anti-β-DG antibodies: after fixation sections were incubated in 0.1 M glycine, 6 M urea, pH 3.5 at 4°C for 1 hour followed by blocking and staining as above. Confocal images were acquired with a Nikon C1 laser scanning confocal attached to a Nikon TE2000 inverted microscope.

Immunofluorescence microscopy of cultured cells

After hormone treatment as described above, cells in Matrigel were gently lifted from plates and spread onto slides, fixed and blocked as above. Cells were incubated with 1:50 rabbit anti-P-STAT5 (Invitrogen) primary antibodies overnight at 4°C. Cells were then washed three times with PBS and incubated for 1 hour at room temperature with 1:50 goat anti-rabbit FITC (Jackson ImmunoResearch) diluted in blocking buffer. Cells were washed three times with PBS, stained with 10 μg/ml propidium iodide, mounted and imaged as above.

Laminin assembly

Fluoroscein-isothiocyanate (FITC)-labeled laminin-111 was prepared as described (Weir et al., 2006). Cells were grown overnight on Lab-Tek II glass chamber slides. FITC-laminin was added at a 10 ng/ml, incubated overnight, and treated cells were fixed with paraformaldehyde. Light and fluorescent microscopy was performed on a TE2000 Nikon inverted microscope with a Photometrics Coolsnap HQ CCD camera controlled with Nikon Elements software. Laminin assembly was quantified by applying the same threshold to the assembled fluorescent laminin images and dividing by the cell area using Metamorph image analysis software. The fluorescence intensity accumulated on DG-knockout cells was then normalized to that on DG-expressing cells to obtain the percentage of normal laminin assembly, where normal assembly=100%.

Real-time quantitative PCR

RT-PCR was performed as described (Xu et al., 2009) using the following primers: GAPDH: forward, 5′-CCCCTGGCCAAGGTCATCCATGAC-3′, reverse, 5′-CATACCAGGAAATGAGCTTGACAAAG-3′; β-Casein: forward, 5′-GCTCAGGCTCAAACCATCTC-3′, reverse, 5′-TGTGGAAGGAAGGGTGCTAC-3′; WAP: forward, 5′-AAAAGCCAGCCCCATTGAGG-3′, reverse, 5′-AGGGTTATCACTGGCACTGG-3′; IGF-1: forward, 5′-TCGTCTTCACACCTCTTCTACCT-3′, reverse, 5′-ACTCATCCACAATGCCTGTCT-3′; E-cadherin: forward, 5′-AATGGCGGCAATGCAATCCCAAGA-3′, reverse, 5′-TGCCACAGACCGATTGTGGAGATA-3′. The Lightcycler PCR protocol was 50°C for 2 minutes, 95°C for 10 minutes, 40 cycles of 95°C for 15 seconds and 60°C for 1 minute. Following amplification, melting curve analysis verified the presence of a single PCR product. Reactions were performed in triplicate and the C_t values normalized to GAPDH expression.

This work was supported by the Department of Defense Breast Cancer Research Program Grant W81XWH-07-1-0416 and National Institute of Health Grant 5R01CA109579. K.P.C. is an Investigator of the Howard Hughes Medical Institute. The authors wish to thank Shruti Nayak for technical assistance and Zena Werb, Armin Akhavan, Marisa Oppizzi, Aejaz Sayeed, and Shan Lu for helpful discussion. Deposited in PMC for release after 6 months.

Supplementary material available online at
http://jcs.biologists.org/cgi/content/full/123/21/3683/DC1

References

Akhtar, N., Marlow, R., Lambert, E., Schatzmann, F., Lowe, E. T., Cheung, J., Katz, E., Li, W., Wu, C., Dedhar, S. et al. (2009). Molecular dissection of integrin signalling proteins in the control of mammary epithelial development and differentiation. *Development* **136**, 1019-1027.

Bao, X., Kobayashi, M., Hatakeyama, S., Angata, K., Gullberg, D., Nakayama, J., Fukuda, M. N. and Fukuda, M. (2009). Tumor suppressor function of laminin-binding alpha-dystroglycan requires a distinct beta3-N-acetylglucosaminyltransferase. *Proc. Natl. Acad. Sci. USA* **106**, 12109-12114.

Barresi, R. and Campbell, K. P. (2006). Dystroglycan: from biosynthesis to pathogenesis of human disease. *J. Cell Sci.* **119**, 199-207.

Beggs, H. E., Schahin-Reed, D., Zang, K., Goebbels, S., Nave, K. A., Gorski, J., Jones, K. R., Sretavan, D. and Reichardt, L. F. (2003). FAK deficiency in cells contributing to the basal lamina results in cortical abnormalities resembling congenital muscular dystrophies. *Neuron* **40**, 501-514.

Beltran-Valero de Bernabe, D., Inamori, K. I., Yoshida-Moriguchi, T., Weydert, C. J., Harper, H. A., Willer, T., Henry, M. D. and Campbell, K. P. (2009). Loss of alpha-dystroglycan laminin binding in epithelium-derived cancers is caused by silencing of large. *J. Biol. Chem.* **284**, 11279-11284.

Bissell, M. J., Radisky, D. C., Rizki, A., Weaver, V. M. and Petersen, O. W. (2002). The organizing principle: microenvironmental influences in the normal and malignant breast. *Differentiation* **70**, 537-546.

Calogero, A., Pavoni, E., Gramaglia, T., D'Amati, G., Ragona, G., Brancaccio, A. and Petrucci, T. C. (2006). Altered expression of alpha-dystroglycan subunit in human gliomas. *Cancer Biol. Ther.* **5**, 441-448.

Cohn, R. D. and Campbell, K. P. (2000). Molecular basis of muscular dystrophies. *Muscle Nerve* **23**, 1456-1471.

Cohn, R. D., Henry, M. D., Michele, D. E., Barresi, R., Saito, F., Moore, S. A., Flanagan, J. D., Skwarchuk, M. W., Robbins, M. E., Mendell, J. R. et al. (2002). Disruption of DAG1 in differentiated skeletal muscle reveals a role for dystroglycan in muscle regeneration. *Cell* **110**, 639-648.

Cotarla, I., Ren, S., Zhang, Y., Gehan, E., Singh, B. and Furth, P. A. (2004). Stat5a is tyrosine phosphorylated and nuclear localized in a high proportion of human breast cancers. *Int. J. Cancer* **108**, 665-671.

Cote, P. D., Moukhles, H., Lindenbaum, M. and Carbonetto, S. (1999). Chimaeric mice deficient in dystroglycans develop muscular dystrophy and have disrupted myoneural synapses. *Nat. Genet.* **23**, 338-342.

Cui, Y., Riedlinger, G., Miyoshi, K., Tang, W., Li, C., Deng, C. X., Robinson, G. W. and Hennighausen, L. (2004). Inactivation of Stat5 in mouse mammary epithelium during pregnancy reveals distinct functions in cell proliferation, survival, and differentiation. *Mol. Cell. Biol.* **24**, 8037-8047.

Dassule, H. R., Lewis, P., Bei, M., Maas, R. and McMahon, A. P. (2000). Sonic hedgehog regulates growth and morphogenesis of the tooth. *Development* **127**, 4775-4785.

Durbeej, M. and Campbell, K. P. (2002). Muscular dystrophies involving the dystrophin-glycoprotein complex: an overview of current mouse models. *Curr. Opin. Genet. Dev.* **12**, 349-361.

Durbeej, M., Henry, M. D., Ferletta, M., Campbell, K. P. and Ekblom, P. (1998). Distribution of dystroglycan in normal adult mouse tissues. *J. Histochem. Cytochem.* **46**, 449-457.

Durbeej, M., Talts, J. F., Henry, M. D., Yurchenco, P. D., Campbell, K. P. and Ekblom, P. (2001). Dystroglycan binding to laminin alpha1LG4 module influences epithelial morphogenesis of salivary gland and lung in vitro. *Differentiation* **69**, 121-134.

Ervasti, J. M. and Campbell, K. P. (1993). A role for the dystrophin-glycoprotein complex as a transmembrane linker between laminin and actin. *J. Cell Biol.* **122**, 809-823.

Esser, A. K., Cohen, M. B. and Henry, M. D. (2010). Dystroglycan is not required for maintenance of the luminal epithelial basement membrane or cell polarity in the mouse prostate. *Prostate* **70**, 777-787.

Graus-Porta, D., Blaess, S., Senften, M., Littlewood-Evans, A., Damsky, C., Huang, Z., Orban, P., Klein, R., Schittny, J. C. and Muller, U. (2001). Beta1-class integrins regulate the development of laminae and folia in the cerebral and cerebellar cortex. *Neuron* **31**, 367-379.

Han, R., Kanagawa, M., Yoshida-Moriguchi, T., Rader, E. P., Ng, R. A., Michele, D. E., Muirhead, D. E., Kunz, S., Moore, S. A., Iannaccone, S. T. et al. (2009). Basal lamina strengthens cell membrane integrity via the laminin G domain-binding motif of {alpha}-dystroglycan. *Proc. Natl. Acad. Sci. USA* **106**, 12573-12579.

Hennighausen, L. and Robinson, G. W. (2008). Interpretation of cytokine signaling through the transcription factors STAT5A and STAT5B. *Genes Dev.* **22**, 711-721.

Henry, M. D. and Campbell, K. P. (1998). A role for dystroglycan in basement membrane assembly. *Cell* **95**, 859-870.

Henry, M. D., Cohen, M. B. and Campbell, K. P. (2001a). Reduced expression of dystroglycan in breast and prostate cancer. *Hum. Pathol.* **32**, 791-795.

Henry, M. D., Satz, J. S., Brakebusch, C., Costell, M., Gustafsson, E., Fassler, R. and Campbell, K. P. (2001b). Distinct roles for dystroglycan, (&bgr;)1 integrin and perlecan in cell surface laminin organization. *J. Cell Sci.* **114**, 1137-1144.

Jonkers, J., Meuwissen, R., van der Gulden, H., Peterse, H., van der Valk, M. and Berns, A. (2001). Synergistic tumor suppressor activity of BRCA2 and p53 in a conditional mouse model for breast cancer. *Nat. Genet.* **29**, 418-425.

Kelly, P. A., Bachelot, A., Kedzia, C., Hennighausen, L., Ormandy, C. J., Kopchick, J. J. and Binart, N. (2002). The role of prolactin and growth hormone in mammary gland development. *Mol. Cell. Endocrinol.* **197**, 127-131.

Klover, P. and Hennighausen, L. (2007). Postnatal body growth is dependent on the transcription factors signal transducers and activators of transcription 5a/b in muscle: a role for autocrine/paracrine insulin-like growth factor I. *Endocrinology* **148**, 1489-1497.

Lee, Y., Kameya, S., Cox, G. A., Hsu, J., Hicks, W., Maddatu, T. P., Smith, R. S., Naggert, J. K., Peachey, N. S. and Nishina, P. M. (2005). Ocular abnormalities in Large(myd) and Large(vls) mice, spontaneous models for muscle, eye, and brain diseases. *Mol. Cell. Neurosci.* **30**, 160-172.

Levedakou, E. N., Chen, X. J., Soliven, B. and Popko, B. (2005). Disruption of the mouse Large gene in the enr and myd mutants results in nerve, muscle, and neuromuscular junction defects. *Mol. Cell. Neurosci.* **28**, 757-769.

Li, N., Zhang, Y., Naylor, M. J., Schatzmann, F., Maurer, F., Wintermantel, T., Schuetz, G., Mueller, U., Streuli, C. H. and Hynes, N. E. (2005). Beta1 integrins regulate mammary gland proliferation and maintain the integrity of mammary alveoli. *EMBO J.* **24**, 1942-1953.

Li, S., Harrison, D., Carbonetto, S., Fassler, R., Smyth, N., Edgar, D. and Yurchenco, P. D. (2002). Matrix assembly, regulation, and survival functions of laminin and its receptors in embryonic stem cell differentiation. *J. Cell Biol.* **157**, 1279-1290.

Liu, X., Robinson, G. W., Wagner, K. U., Garrett, L., Wynshaw-Boris, A. and Hennighausen, L. (1997). Stat5a is mandatory for adult mammary gland development and lactogenesis. *Genes Dev.* **11**, 179-186.

Markham, K., Schuurmans, C. and Weiss, S. (2007). STAT5A/B activity is required in the developing forebrain and spinal cord. *Mol. Cell. Neurosci.* **35**, 272-282.

Martin, L. T., Glass, M., Dosunmu, E. and Martin, P. T. (2007). Altered expression of natively glycosylated alpha dystroglycan in pediatric solid tumors. *Hum. Pathol.* **38**, 1657-1668.

Miner, J. H. and Yurchenco, P. D. (2004). Laminin functions in tissue morphogenesis. *Annu. Rev. Cell Dev. Biol.* **20**, 255-284.

Miyagoe, Y., Hanaoka, K., Nonaka, I., Hayasaka, M., Nabeshima, Y., Arahata, K., Nabeshima, Y. and Takeda, S. (1997). Laminin alpha2 chain-null mutant mice by targeted disruption of the Lama2 gene: a new model of merosin (laminin 2)-deficient congenital muscular dystrophy. *FEBS Lett.* **415**, 33-39.

Moore, S. A., Saito, F., Chen, J., Michele, D. E., Henry, M. D., Messing, A., Cohn, R. D., Ross-Barta, S. E., Westra, S., Williamson, R. A. et al. (2002). Deletion of brain dystroglycan recapitulates aspects of congenital muscular dystrophy. *Nature* **418**, 422-425.

Muntoni, F., Torelli, S. and Brockington, M. (2008). Muscular dystrophies due to glycosylation defects. *Neurotherapeutics* **5**, 627-632.

Muschler, J., Lochter, A., Roskelley, C. D., Yurchenco, P. and Bissell, M. J. (1999). Division of labor among the alpha6beta4 integrin, beta1 integrins, and an E3 laminin receptor to signal morphogenesis and beta-casein expression in mammary epithelial cells. *Mol. Biol. Cell* **10**, 2817-2828.

Muschler, J., Levy, D., Boudreau, R., Henry, M., Campbell, K. and Bissell, M. J. (2002). A role for dystroglycan in epithelial polarization: loss of function in breast tumor cells. *Cancer Res.* **62**, 7102-7109.

Nagy, T., Wei, H., Shen, T. L., Peng, X., Liang, C. C., Gan, B. and Guan, J. L. (2007). Mammary epithelial-specific deletion of the focal adhesion kinase gene leads to severe lobulo-alveolar hypoplasia and secretory immaturity of the murine mammary gland. *J. Biol. Chem.* **282**, 31766-31776.

Naylor, M. J., Li, N., Cheung, J., Lowe, E. T., Lambert, E., Marlow, R., Wang, P., Schatzmann, F., Wintermantel, T., Schuetz, G. et al. (2005). Ablation of beta1 integrin in mammary epithelium reveals a key role for integrin in glandular morphogenesis and differentiation. *J. Cell Biol.* **171**, 717-728.

Niewmierzycka, A., Mills, J., St-Arnaud, R., Dedhar, S. and Reichardt, L. F. (2005). Integrin-linked kinase deletion from mouse cortex results in cortical lamination defects resembling cobblestone lissencephaly. *J. Neurosci.* **25**, 7022-7031.

Nishimune, H., Valdez, G., Jarad, G., Moulson, C. L., Muller, U., Miner, J. H. and Sanes, J. R. (2008). Laminins promote postsynaptic maturation by an autocrine mechanism at the neuromuscular junction. *J. Cell Biol.* **182**, 1201-1215.

Oakes, S. R., Rogers, R. L., Naylor, M. J. and Ormandy, C. J. (2008). Prolactin regulation of mammary gland development. *J. Mammary Gland Biol. Neoplasia* **13**, 13-28.

Philp, J. A., Burdon, T. G. and Watson, C. J. (1996). Differential activation of STATs 3 and 5 during mammary gland development. *FEBS Lett.* **396**, 77-80.

Reed, U. C. (2009). Congenital muscular dystrophy. Part II: a review of pathogenesis and therapeutic perspectives. *Arq. Neuropsiquiatr.* **67**, 343-362.

Robinson, G. W. (2007). Cooperation of signalling pathways in embryonic mammary gland development. *Nat. Rev. Genet.* **8**, 963-972.

Satz, J. S., Barresi, R., Durbeej, M., Willer, T., Turner, A., Moore, S. A. and Campbell, K. P. (2008). Brain and eye malformations resembling Walker-Warburg syndrome are recapitulated in mice by dystroglycan deletion in the epiblast. *J. Neurosci.* **28**, 10567-10575.

Sgambato, A., Migaldi, M., Montanari, M., Camerini, A., Brancaccio, A., Rossi, G., Cangiano, R., Losasso, C., Capelli, G., Trentini, G. P. et al. (2003). Dystroglycan expression is frequently reduced in human breast and colon cancers and is associated with tumor progression. *Am. J. Pathol.* **162**, 849-860.

Sgambato, A., Camerini, A., Faraglia, B., Pavoni, E., Montanari, M., Spada, D., Losasso, C., Brancaccio, A. and Cittadini, A. (2004). Increased expression of dystroglycan inhibits the growth and tumorigenicity of human mammary epithelial cells. *Cancer Biol. Ther.* **3**, 967-975.

Singh, J., Itahana, Y., Knight-Krajewski, S., Kanagawa, M., Campbell, K. P., Bissell, M. J. and Muschler, J. (2004). Proteolytic enzymes and altered glycosylation modulate dystroglycan function in carcinoma cells. *Cancer Res.* **64**, 6152-6159.

Soriano, P. (1999). Generalized lacZ expression with the ROSA26 Cre reporter strain. *Nat. Genet.* **21**, 70-71.

Streuli, C. H., Schmidhauser, C., Bailey, N., Yurchenco, P., Skubitz, A. P., Roskelley, C. and Bissell, M. J. (1995). Laminin mediates tissue-specific gene expression in mammary epithelia. *J. Cell Biol.* **129**, 591-603.

Tan, S. H. and Nevalainen, M. T. (2008). Signal transducer and activator of transcription 5A/B in prostate and breast cancers. *Endocr. Relat. Cancer* **15**, 367-390.

Wagner, K. U., Young, W. S., 3rd, Liu, X., Ginns, E. I., Li, M., Furth, P. A. and Hennighausen, L. (1997). Oxytocin and milk removal are required for post-partum mammary-gland development. *Genes Funct.* **1**, 233-244.

Wagner, K. U., Krempler, A., Triplett, A. A., Qi, Y., George, N. M., Zhu, J. and Rui, H. (2004). Impaired alveologenesis and maintenance of secretory mammary epithelial cells in Jak2 conditional knockout mice. *Mol. Cell. Biol.* **24**, 5510-5520.

Weir, M. L., Oppizzi, M. L., Henry, M. D., Onishi, A., Campbell, K. P., Bissell, M. J. and Muschler, J. L. (2006). Dystroglycan loss disrupts polarity and β-casein induction in mammary epithelial cells by perturbing laminin anchoring. *J. Cell Sci.* **119**, 4047-4058.

Xu, R., Nelson, C. M., Muschler, J. L., Veiseh, M., Vonderhaar, B. K. and Bissell, M. J. (2009). Sustained activation of STAT5 is essential for chromatin remodeling and maintenance of mammary-specific function. *J. Cell Biol.* **184**, 57-66.

Yoshida-Moriguchi, T., Yu, L., Stalnaker, S. H., Davis, S., Kunz, S., Madson, M., Oldstone, M. B., Schachter, H., Wells, L. and Campbell, K. P. (2010). O-mannosyl phosphorylation of alpha-dystroglycan is required for laminin binding. *Science* **327**, 88-92.

Yurchenco, P. D. and Patton, B. L. (2009). Developmental and pathogenic mechanisms of basement membrane assembly. *Curr. Pharm. Des.* **15**, 1277-1294.

Yurchenco, P. D., Amenta, P. S. and Patton, B. L. (2004). Basement membrane assembly, stability and activities observed through a developmental lens. *Matrix Biol.* **22**, 521-538.

Dystroglycan controls signaling of multiple hormones through modulation of STAT5 activity
J Cell Sci Leonoudakis et al. 123: 3683

JCS070680 Supplementary Material

Files in this Data Supplement:

- **Supplemental Figure 1** -

Fig. S1. K14-Cre expression might be initiated as early as E13 in mammary gland development. Histochemical staining for *lacZ* expression, performed in bi-transgenic K14-Cre^{+}; R26R^{+} mice, appears to reveal K14-Cre-mediated DNA recombination in the mammary gland nodes (black arrows) at the E13 stage of development just before broader activation of K14-Cre expression in the epidermis at E13.5 (Jonkers et al., 2001). The forelimb (open arrows) lies adjacent to the nodes. Scale bar: 1 mm.

- **Supplemental Figure 2** -

Fig. S2. Rosa26R reporter activity is evident throughout the epithelium in mammary glands of ΔDGK14-Cre mice. Histochemical staining for *lacZ* expression in lactating ΔDG$^{K14\text{-}Cre}$;R26R^{+} mice demonstrates K14-Cre-mediated DNA recombination. (A) At lactation day 1 (L1), *lacZ* reporter activity is absent from control (Cre^{-}) mice. (B) Abundant *lacZ* reporter activity (blue) is evident in ΔDG$^{K14\text{-}Cre}$;R26R^{+} mammary tissue sections showing *lacZ* expression in the epithelium. (C) Enlargement of boxed area in B shows *lacZ* expression in luminal as well as myoepithelial cell populations. Scale bars: 50 μm.

- **Supplemental Figure 3** -

Fig. S3. Pups from ΔDG$^{K14\text{-}Cre}$ mothers do not receive adequate nourishment. Compared with control mice, mouse pups from ΔDG$^{K14\text{-}Cre}$ mothers failed to obtain adequate nourishment indicated by the lack of a milk spot in the stomach (arrow), emaciated appearance and high rate of mortality.

- **Supplemental Figure 4** -

Fig. S4. Mammary gland outgrowth is attenuated in lactating ΔDG$^{K14\text{-}Cre}$ mice. Mammary gland development in several control and ΔDG$^{K14\text{-}Cre}$ mice was assessed by whole-mount staining of the fourth (inguinal) gland. Glands were either stained by carmine allum (red) or X-gal (blue) to reveal Cre activity on the Rosa26R transgene. At lactation day 1, control glands showed normal tissue architecture, whereas ΔDG$^{K14\text{-}Cre}$ glands displayed an apparent reduction in outgrowth. Scale bars: 1 mm (top), 100 μm (bottom).

- **Supplemental Figure 5** -

Fig. S5. Expression of milk proteins and mRNA transcripts in ΔDG$^{K14\text{-}Cre}$ mice is not significantly perturbed. (A) Protein extracts from mammary glands taken from L1 stage control and ΔDG$^{K14\text{-}Cre}$ mice were resolved by SDS-PAGE, transferred to PVDF, and immunoblotted with the antibodies for the milk proteins indicated at the right of the blots. E-cadherin was used as a loading control for epithelia within the gland. Mouse number indicates the number given to individual mice for genotyping. (B) β-casein, whey acidic protein (WAP) and E-cadherin mRNA transcript levels were measured by qPCR. β-casein and WAP C_t values were then divided by E-cadherin C_t values to normalize for the epithelial content in each sample. Ratios from ΔDG$^{K14\text{-}Cre}$ (KO; n=4) and control (WT; n=3) mice were averaged and graphed. Error bars represent s.d.

- **Supplemental Figure 6** -

Fig. S6. Laminin deposition and tissue architecture appear unchanged after the knockout of dystroglycan expression by K14-Cre. (A) Tissue sections of L1 stage mammary glands from control and ΔDG$^{K14\text{-}Cre}$ mice were immunostained with

antibodies to the apical marker ZO-1 and basal marker α6-integrin. (B) L1 stage mammary gland sections were stained with antibodies against the myoepithelial cell markers keratin-14 (K14) and anti-α-smooth muscle actin (ASMA). (C) Laminin expression and deposition was assessed by immunostaining for laminin in glands from lactating animals; E-cadherin staining marks the epithelial cells. Scale bars: 20 μm.

- **Supplemental Figure 7** -

Fig. S7. DG modulates STAT5 activity in nulliparous mice. (A) Tissue sections of nulliparous mammary glands from control or $\Delta DG^{K14\text{-}Cre}$ mice were immunostained with anti-STAT5 antibodies and counterstained with propidium iodide to stain the nuclei. $\Delta DG^{K14\text{-}Cre}$ mammary glands show markedly reduced nuclear STAT5 staining as indicated by the arrows and by the lack of overlap staining (yellow color) in the merged images at right. (B) Tissue sections of nulliparous mammary glands from control or $\Delta DG^{K14\text{-}Cre}$ mice were immunostained with anti-STAT5-*P* antibodies and counterstained with propidium iodide to stain the nuclei. Phosphorylated STAT5 staining in $\Delta DG^{K14\text{-}Cre}$ mammary glands was absent. Scale bar: 20 μm.

- **Supplemental Figure 8** -

Fig. S8. Evaluation of STAT3 activity shows no evidence of premature involution in $\Delta DG^{K14\text{-}Cre}$ mice. Protein extracts from mammary glands taken from L1 stage control and $\Delta DG^{K14\text{-}Cre}$ mice were resolved by SDS-PAGE, transferred to PVDF, and immunoblotted with the antibodies for phosphorylated STAT3 and total STAT3. Actin expression was used as a loading control. Mouse number indicates the number given to individual mice for genotyping.

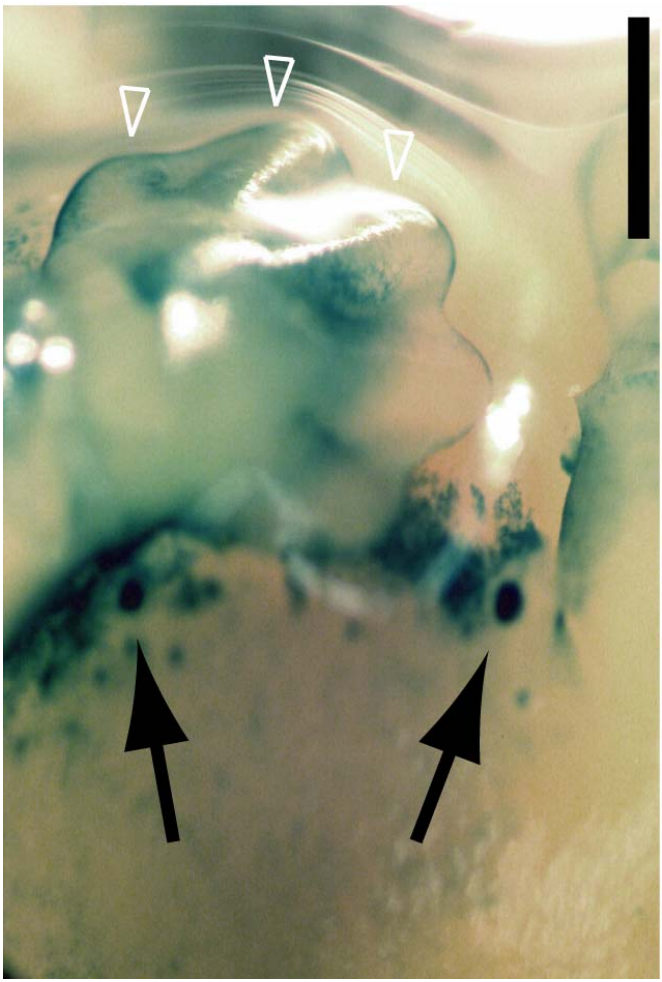

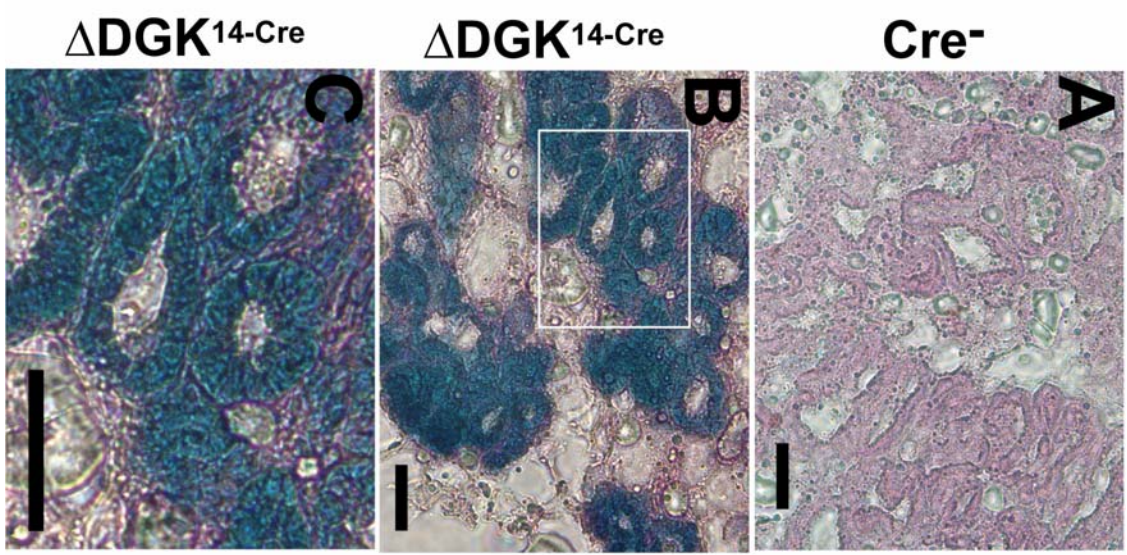
ΔDGK14-Cre
ΔDGK14-Cre
Cre-
C
B
A

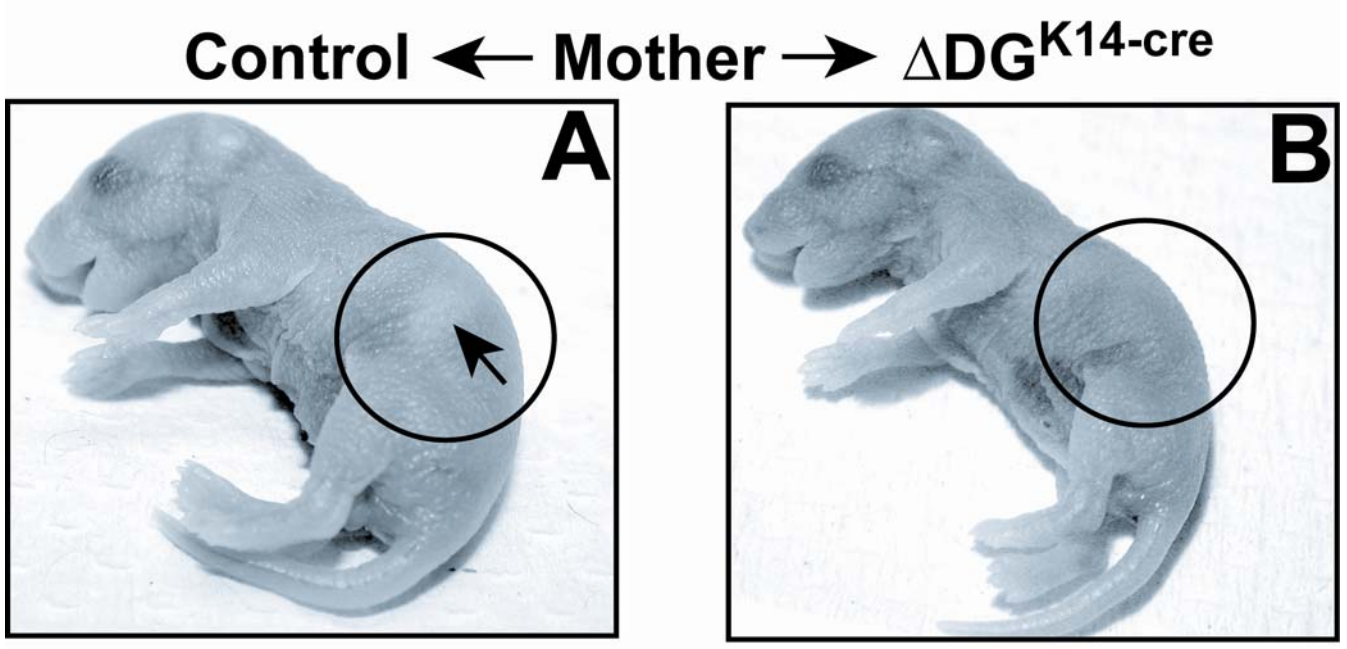
Control ← Mother → ΔDG^K14-cre
A
B

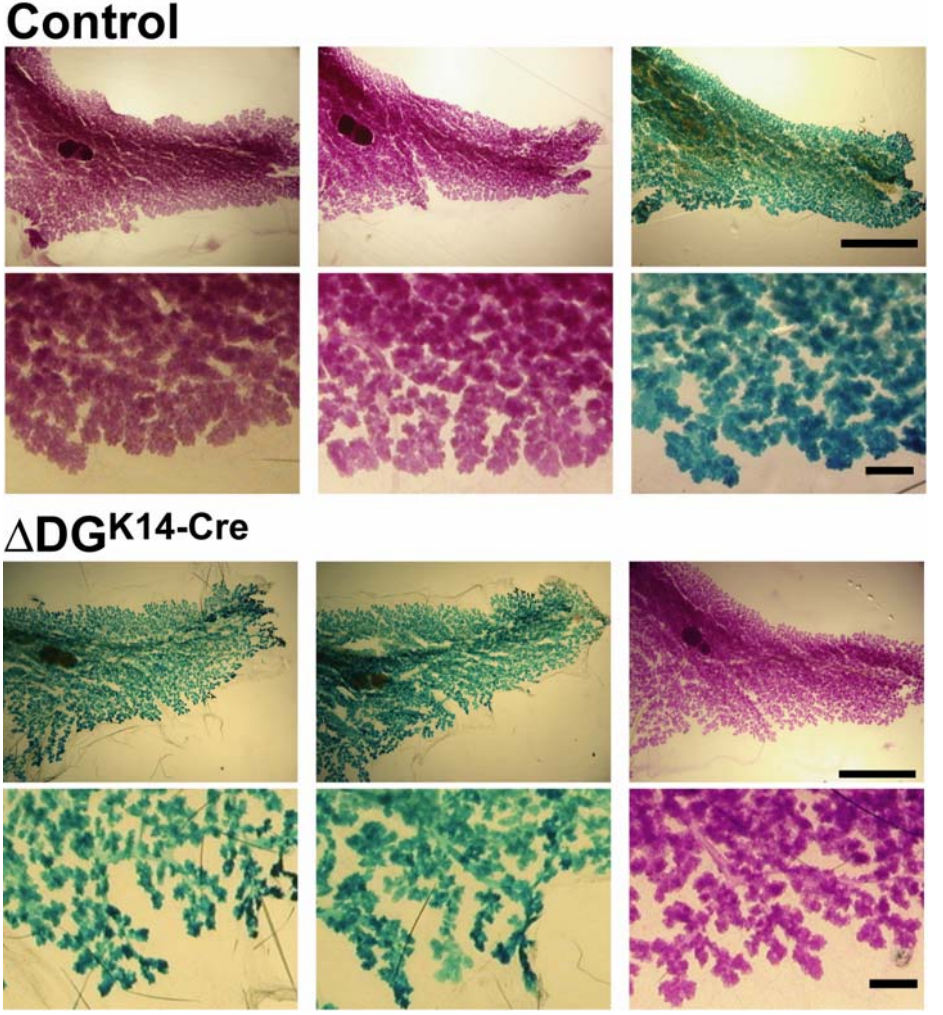
Control
ΔDGK14-Cre

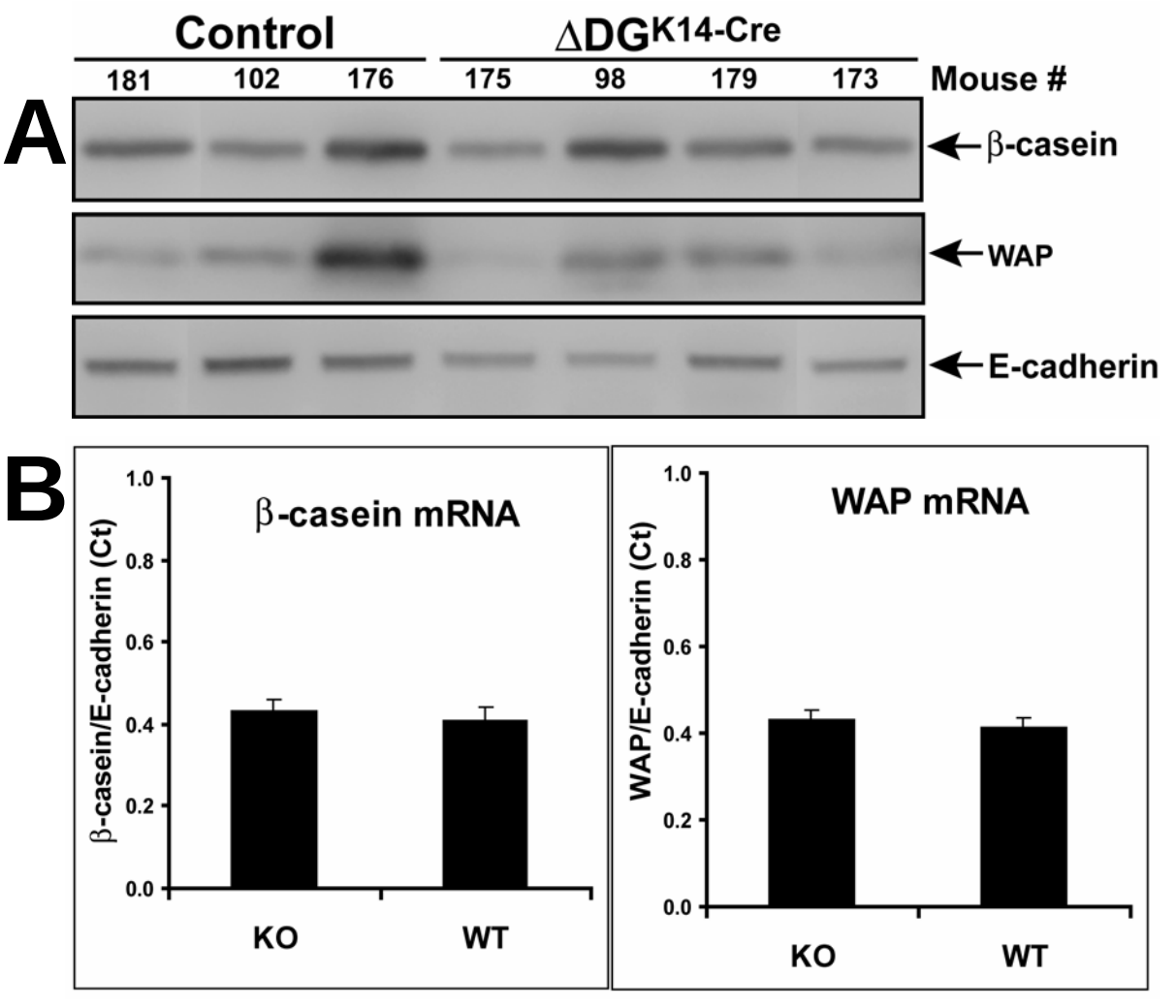
A
Control
ΔDGK14-Cre
181
102
176
175
98
179
173
Mouse #
β-casein
WAP
E-cadherin
B
β-casein mRNA
β-casein/E-cadherin (Ct)
1.0
0.8
0.6
0.4
0.2
0.0
KO
WT
WAP mRNA
WAP/E-cadherin (Ct)
1.0
0.8
0.6
0.4
0.2
0.0
KO
WT

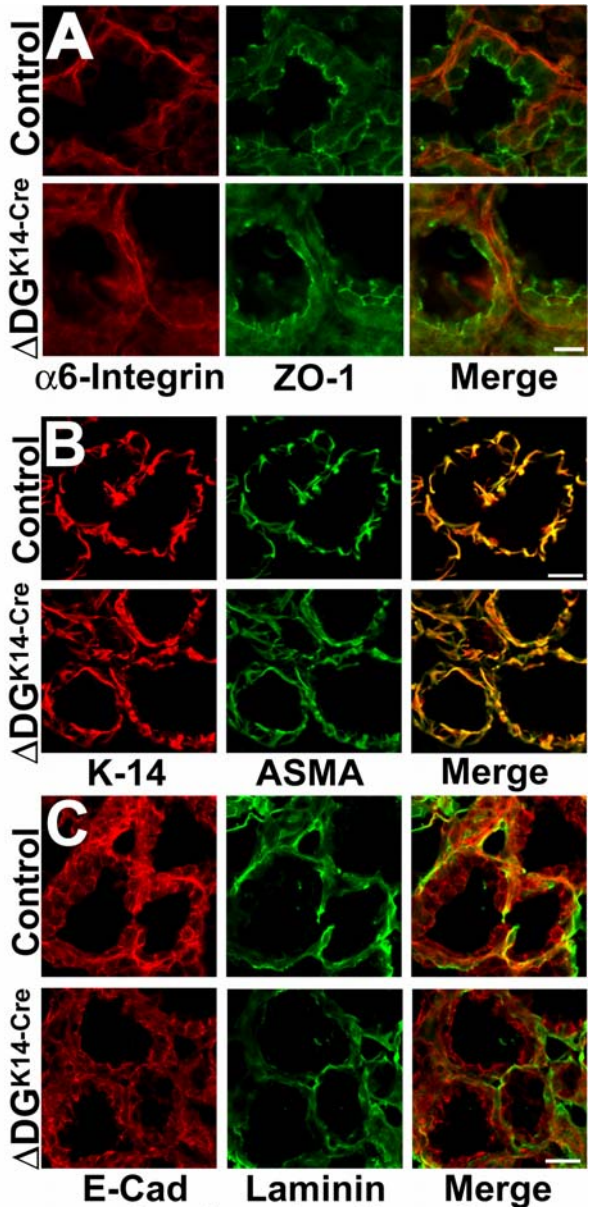
A
Control
ΔDGK14-Cre
α6-Integrin
ZO-1
Merge
B
Control
ΔDGK14-Cre
K-14
ASMA
Merge
C
Control
ΔDGK14-Cre
E-Cad
Laminin
Merge

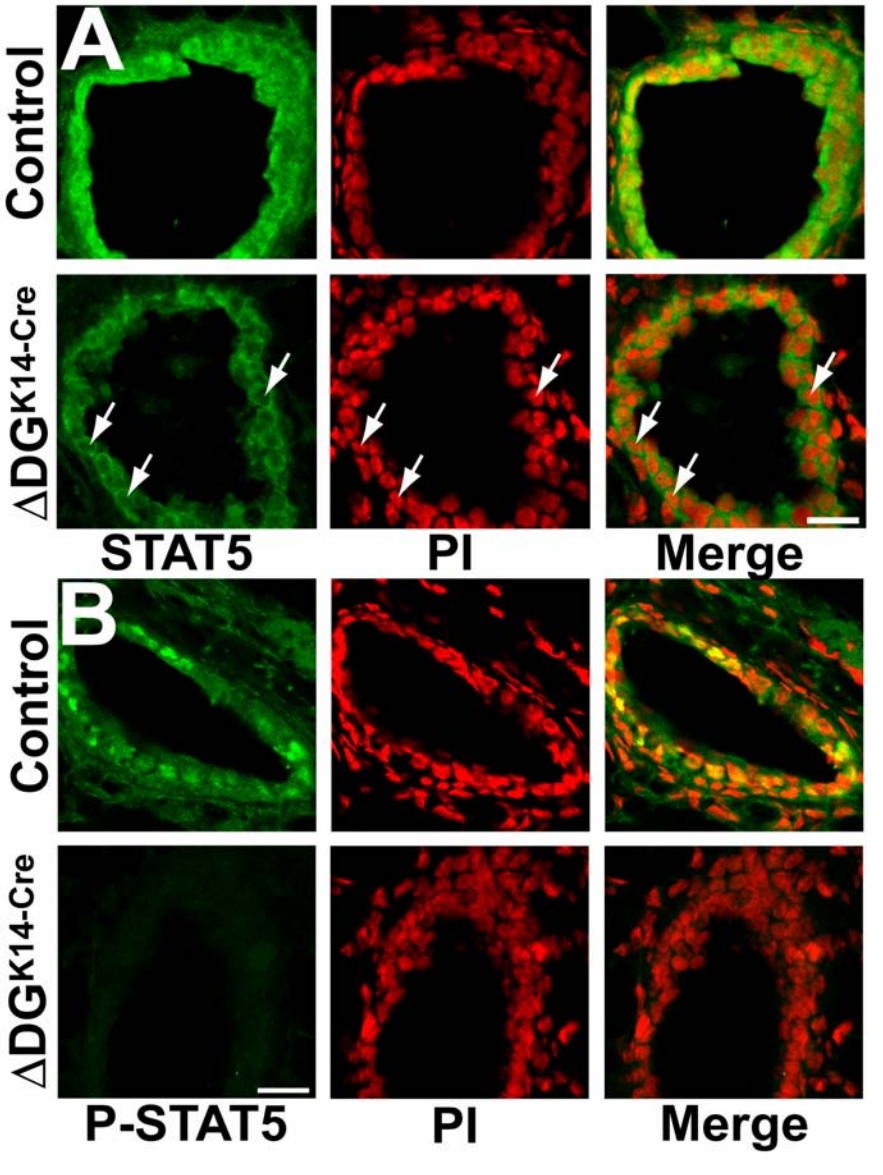
A
Control
ΔDGK14-Cre
STAT5
PI
Merge
B
Control
ΔDGK14-Cre
P-STAT5
PI
Merge

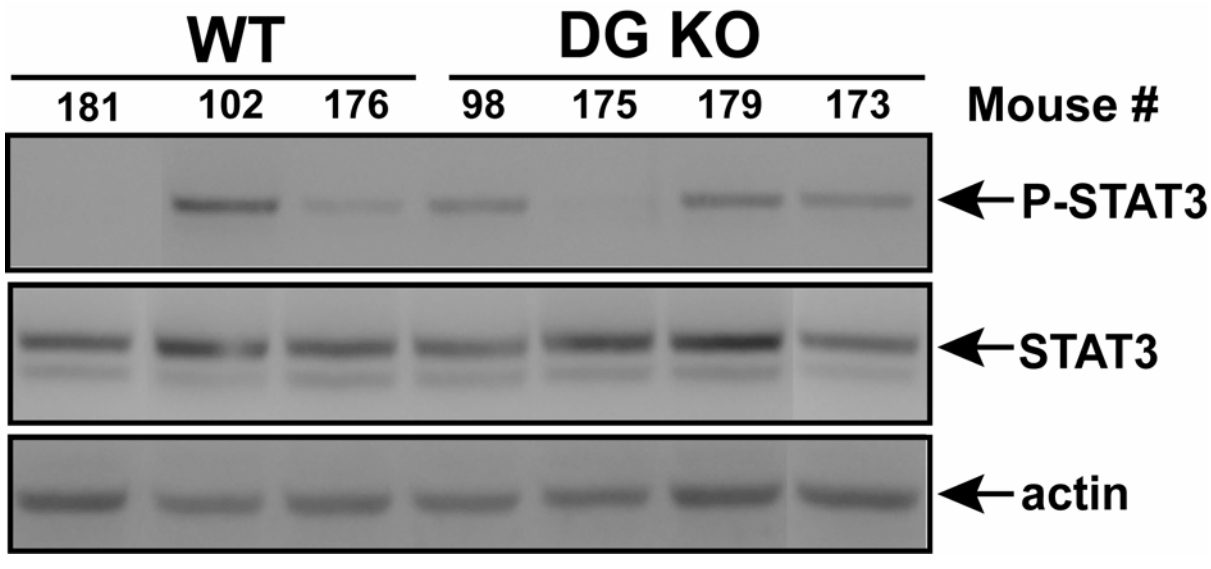
WT
DG KO
181
102
176
98
175
179
173
Mouse #
P-STAT3
STAT3
actin